Environmental Science & Technology

Article

pubs.acs.org/est

A Novel Exposure System Termed NAVETTA for In Vitro Laminar Flow Electrodeposition of Nanoaerosol and Evaluation of Immune Effects in Human Lung Reporter Cells

Evelien Frijns,[†] Sandra Verstraelen,[†] Linda Corinna Stoehr,[‡] Jo Van Laer,[†] An Jacobs,[†] Jan Peters,[†] Kristof Tirez,[†] Matthew Samuel Powys Boyles,[‡] Mark Geppert,[‡] Pierre Madl,[‡] Inge Nelissen,[†] Albert Duschl,[‡] and Martin Himly*[,‡]

[†]Flemish Institute for Technological Research (VITO NV), Boeretang 200, 2400 Mol, Belgium

[‡]Paris Lodron University of Salzburg (PLUS), Department of Molecular Biology, Hellbrunnerstrasse 34, 5020 Salzburg, Austria

Supporting Information

ABSTRACT: A new prototype air–liquid interface (ALI) exposure system, a flatbed aerosol exposure chamber termed NAVETTA, was developed to investigate deposition of engineered nanoparticles (NPs) on cultured human lung A549 cells directly from the gas phase. This device mimics human lung cell exposure to NPs due to a low horizontal gas flow combined with cells exposed at the ALI. Electrostatic field assistance is applied to improve NP deposition efficiency. As proof-of-principle, cell viability and immune responses after short-term exposure to nanocopper oxide (CuO)-aerosol were determined. We found that, due to the laminar aerosol flow and a specific orientation of inverted transwells, much higher deposition rates were obtained compared to the normal ALI setup. Cellular responses were monitored with postexposure incubation in submerged conditions, revealing CuO dissolution in a concentration-dependent manner. Cytotoxicity was the result of ionic and nonionic Cu fractions. Using the optimized inverted ALI/postincubation procedure, pro-inflammatory immune responses, in terms of *interleukin (IL)-8* promoter and nuclear factor kappa B (NFκB) activity, were observed within short time, i.e. One hour exposure to ALI-deposited CuO-NPs and 2.5 h postincubation. NAVETTA is a novel option for mimicking human lung cell exposure to NPs, complementing existing ALI systems.

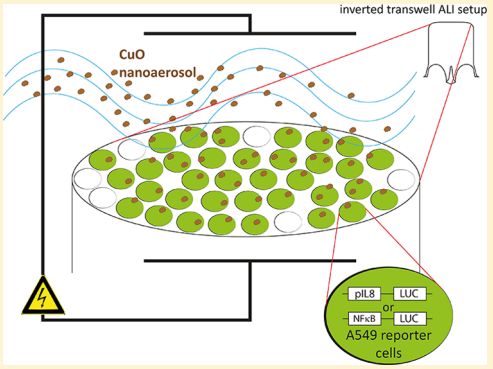

INTRODUCTION

To overcome the deficiencies of nanotoxicity testing approaches in inhalation toxicology using submerged in vitro biological models, as reviewed by Paur and co-workers,[1] several in vitro systems have been developed for exposure of cells at the air–liquid interface (ALI) to aerosolized nanoparticles (NPs). This allows for a more realistic interaction between pulmonary cells and NPs, limits alterations of the physicochemical properties of the NPs, and provides a more accurate dose determination.[2]

The available systems are based on different mechanisms of aerosol delivery, including diffusion,[3−8] gravitational cloud settling,[6] impaction (CULTEX/VITROCELL),[3−5,9,10] electrostatic deposition[11−13] or a combination thereof.[14] They have been used to investigate biological effects of a variety of aerosols, ranging from combustion-derived particles, such as diesel exhaust aerosol (DEA),[4,13,15−22] cigarette smoke,[23,24] and incinerator fly ash,[5] to engineered NP aerosols generated from nebulized suspensions or dry powders.[6,7,25−33]

The majority of ALI experiments based on diffusion and/or gravitational settling as deposition mechanisms typically have shown a relatively low deposition.[3−8] At a later stage, electrostatic precipitation for uni- or bipolar charged particles has been introduced as one of the main mechanism to improve deposition efficiency.[11−13,34,35] In these systems the aerosol is applied either via a vertical flow directly onto the cell cultures or using a horizontal laminar flow and an electrostatic field generated by placing electrodes beneath the cell cultures, which substantially increases deposition efficiencies, but still requires exposure times of several hours. Referring to existing ALI-exposure devices, increasing the flow rate would lead to increased cell damage due to drying effects or shear stress, so other approaches should be explored.

Physical laws suggest that minimizing the distance the particles have to be deflected from the direction of the flow before they deposit onto the cells can help to further improve deposition efficiency and reduce the introduction of turbulences in the laminar airflow, while simultaneously keeping the time of exposure low. Using an approach previously described by Holder et al.[29] in which the cells are seeded on the reverse side of a transwell insert membrane and the inserts are placed

Received: January 26, 2017
Revised: March 16, 2017
Accepted: March 24, 2017
Published: March 24, 2017

DOI: 10.1021/acs.est.7b00493
Environ. Sci. Technol. 2017, 51, 5259−5269

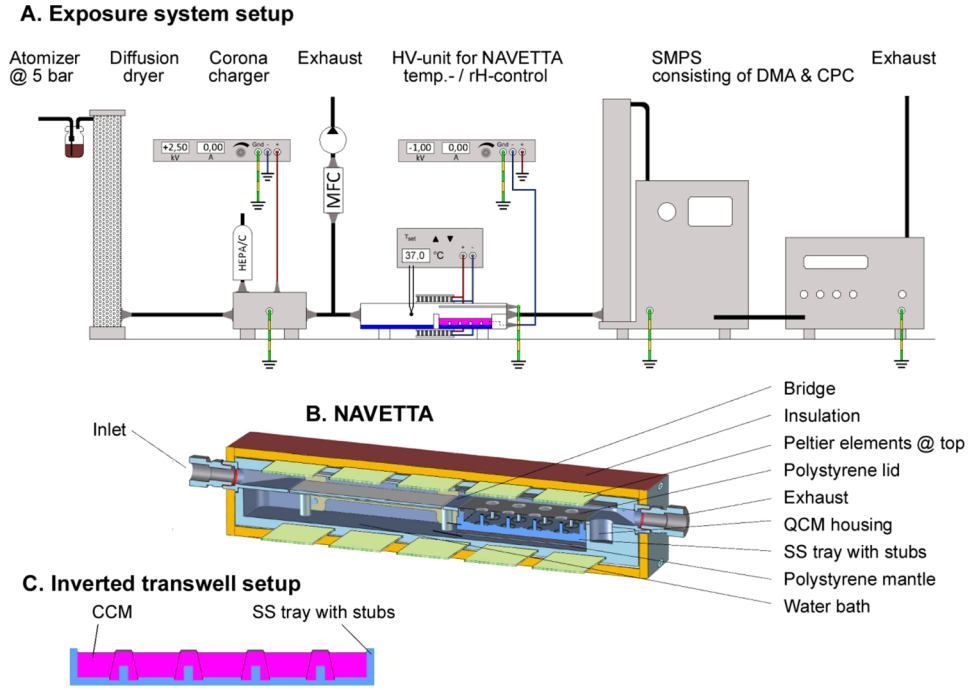

Figure 1. Schematic diagram of aerosolization setup in fume hood with details like atomizer, dryer, carbon/HEPA filter unit (HEPA/C), corona charger, mass flow controller (MFC), and novel exposure chamber (NAVETTA) operating with inverted transwell ALI setup for electrostatic field (EF)-assisted laminar flow deposition of humidified/temperature-controlled nanoaerosol using high voltage (HV), quartz crystal microbalance (QCM), scanning mobility particle sizer (SMPS), condensation particle counter (CPC), stainless steel (SS) tray, cell culture medium (CCM).

in an inverted position into the exposure chamber, this distance can be reduced significantly compared to the normal hanging setup increasing the likelihood of contact between particles and cells. Furthermore, as recently shown in a study investigating DEA-induced biological responses,[13] well-controlled exposure conditions (specifically temperature and relative humidity) are of utmost importance to maintain cellular functionality.

In the present study, a new in-house ALI exposure module has been developed. This device has an added value to existing ALI systems in terms of (1) highly efficient laminar flow electrostatic deposition of NPs onto cells requiring, (2) brief exposure times, and (3) simple, rapid detection of cell viability and in vitro pro-inflammatory effects of NPs using the A549 reporter lines pIL8-luc and NFκB-luc. Reporter cells offer alternatives to replace complex experimental procedures with often low throughput, limited parallel measurements, and long processing times,[36−38] and they have previously been used as cell-based biosensors in nanotoxicological research.[39,40] Both suitability and experimental handling of these cell lines for ALI-experiments have already been described in detail.[13,32] As proof-of-principle, cell viability and immune responses after short-term exposure to a nanoaerosol generated from copper oxide (CuO)-NPs were determined.

Among the manufactured metal oxide NPs, CuO-NPs are increasingly used in industrial catalysis[41] as components of gas sensors,[42] batteries,[43] solar energy converters,[44] high-temperature superconductors and field emitters.[45] CuO-NPs are also used for their antimicrobial activity with possible applications to disposable textiles or food containers.[46] The toxic effects and mechanisms of CuO-NPs are reviewed by Chang et al.[47] Briefly, Cu is an indispensable element for maintaining homeostasis in organisms.[48] Cu may cause toxicity once the concentration exceeds the physiological tolerance range in vivo.[49] Toxicity assessment studies working with CuO-NPs have focused on investigating the effects of different exposure routes, such as the respiratory or gastrointestinal tract. In vivo studies described lung toxicity of CuO-NPs after intratracheal instillation in rats.[50] Several in vitro studies investigated the potential toxic effects of CuO-NPs, mainly on airway epithelial (Hep-2) cells and alveolar epithelial (A549) cells. CuO-NPs were shown to trigger the production of reactive oxygen species (ROS), to induce generation of oxidative stress and DNA damage, to block cellular antioxidant defenses[51−56] and to induce mitochondrial depolarisation in A549 cells.[57] CuO-NPs also induced concentration- and time-dependent cytotoxicity, and elicited a permeability and inflammation response in human cardiac microvascular endothelial cells[58] and differentiated Caco-2 intestinal cell monolayers.[59] The high cytotoxicity is most likely related to particle characteristics like the high surface area, which may facilitate redox reactions either intra- or extracellularly, inducing cell death. Besides the particle effect, Cu-ions released extracellularly may also contribute to the cytotoxicity.[59−61] In contrast, some authors state that CuO-NPs toxicity is not dependent on Cu-ions released by NPs.[54,56]

Briefly, this study describes the development of a novel ALI exposure module, termed NAVETTA, allowing simple and rapid detection of cell viability and in vitro pro-inflammatory responses upon engineered NP exposure of human lung epithelial A549 reporter cells grown in inverted transwell setup. Furthermore, objectives included a high efficient uniform deposition mediated by electrostatic field from a low laminar nanoaerosol flow.

MATERIALS AND METHODS

Methodological details on the physicochemical characterization of the CuO-NPs bulk material, dispersion, generated nano-

DOI: 10.1021/acs.est.7b00493
Environ. Sci. Technol. 2017, 51, 5259−5269

aerosol, and deposited material are described in the Supporting Information (SI).

Aerosolization Setup. Nanoaerosols were generated using a collision-type atomizer (model ATM 220, Topas, Dresden, Germany) containing a 50 mL CuO suspension and HEPA-filtered laboratory compressed air (5 bar). Synthetic CuO-NPs of 22−25 nm (Nanologica AB) were dispersed in Milli-Q water to prepare a CuO-NP suspension (4 g/L). The bulk material of CuO powder used for generating the nanoaerosol was provided by Intrinsiq Materials Ltd. (Farnborough, UK). The suspension was sonicated in conformity with the standard operating procedure (SOP) *"Dispersion of NNV-011 (CuO) nanoparticle suspensions for in vitro toxicological testing"* developed by the NanoValid consortium (publicly available from www.nanovalid.eu) was immediately used for atomization. The NP-containing air flow leaving the atomizer (at 4 L per minute, lpm) was dried using a diffusion dryer (Figure 1A). A second air flow of 1 Lpm laboratory compressed air passed through a carbon and HEPA filter (HEPA/C) and an ionizer (corona jet charger, operated at +2.5 kV). Both flow streams were merged in a mixing chamber where particles in the aerosol flow mixed with the positive ions carried by the filtered clean air. Using a T-split junction, 0.3 lpm of the charged aerosol flow entered the NAVETTA, while 4.7 lpm were led into the exhaust of the fume hood using a pump connected to a mass flow controller (MFC). The exhaust of the exposure chamber was connected to a scanning mobility particle sizer (SMPS, model 3936L25, TSI Inc., Shoreview, MN) that incorporates both a dynamic mobility analyzer (DMA) and a condensation particle counter (CPC) operating at a sample flow of 0.3 Lpm measuring in the size range of 15−661 nm.

NAVETTA Exposure Chamber. The prototype flatbed aerosol exposure chamber (45 cm length, 11 cm width, 5.5 cm height) termed "NAVETTA" was constructed of an anodized aluminum chassis (Figure 1B). A European Patent entitled *"Flatbed air-liquid interface exposure module and methods"* was filed on November 24, 2016 under application number EP16200571.4 in name of VITO NV and PLUS. Temperature control was achieved by five equidistantly placed Peltier elements (with a power rating of 90 W each) on the upper lid and likewise five at the lower lid of the NAVETTA. The Peltier elements were operated either in heating- or cooling-mode via an external controller with a built-in temperature sensor. To ensure stable thermal conditions (36−37 °C), the chamber was embedded in a ruggedized polyethylene housing, allowing only the polyethylene to be in contact with the outside mounted heat sink. The upper lid could be removed for easy access to the inverted transwell cell culture. The inside of NAVETTA consisted of three compartments: the first compartment after the aerosol inlet represented a water bath, filled with 50 mL of Milli-Q water, to humidify the aerosol stream; the second compartment was designed to house a stainless steel (SS) tray containing cell culture medium (CCM) with studs to position 12 inverted transwell inserts; in the third compartment, a gravimetric sensor (quartz crystal microbalance, QCM, Novaetech s.r.l., Napoli, Italy) was fitted into the metallic chassis along with a temperature and humidity sensor (thin humidity probe model 0636 2135 combined with thermohygrometer 635-2, Testo, Lenzkirch, Germany) to monitor air quality inside the chamber. Temperature, relative humidity (rH), and mass data were logged via an Arduino-based software interface to an external computer.

To enable electrostatic field (EF)-assisted deposition of the positively charged CuO nanoaerosols onto the inverted transwell cell-inserts (Figure 1C), the SS tray was connected to a high-voltage (HV) source (−1 kV, with the current control set to minimum). The grounded counter-electrode was integrated into the upper lid directly above the SS tray. For electric insulation from both the water bath holding the plate and the aluminum housing, the SS tray was placed into a 1 mm thick polystyrene mantle. To shield the CCM-containing SS tray from the charged CuO-nanoaerosol, a polystyrene top-lid with 12 well-designed tight openings of 15 mm was used. In this way, the charged CuO-nanoaerosol was more precisely oriented onto the air-lifted cell monolayers, thereby avoiding losses of aerosol through deposition in the intermediate spaces. A scheme of the whole aerosolization and deposition setup is shown in Figure 1.

Cell Lines and Culture Conditions. Two A549 (human alveolar epithelial lung carcinoma) reporter cell lines were used, possessing a luciferase reporter gene (luc) under the regulation of the promoter of interleukin (IL)-8 (pIL8-luc) or under regulation of four copies of the nuclear factor kappa B (NFκB) response element (NFκB-luc). The establishment of these cell lines has been described in detail.[62] Cell culture conditions and analysis of the biological end points (cell viability and immune response) including statistical analysis are described in the SI.

ALI Exposure. For each analysis (i.e., Cu quantification using ICP-MS, cell viability, pro-inflammatory potential), 12 transwell inserts were exposed to clean air (vehicle control; that is, carbon- and HEPA-filtered laboratory compressed air), to 12 ppm nitrogen dioxide (NO_2, positive control for cell viability) from a gas cylinder, and to 4 g/L aerosolized CuO-NPs for an exposure period of 1 h (0.3 lpm, + 2.5 kV corona charger, −1 kV HV). Temperature and rH during exposure were monitored and found to be stable at 36−37 °C and 99% rH, which thus achieved the intended agreement with the situation in human lungs. After 1 h exposure, the biological end point measurements and Cu quantification were conducted. Three independent biological experiments using different passages (#3−9) of the cell lines and freshly made CuO-NP suspensions were performed.

At least three incubator controls, that is, negative control cultures that were left to stand in the incubator during exposure, were included in each biological experiment. For this, inserts were placed in a humidified incubator for 1 h in inverted position in a tray containing 5.5 mL CCM/well. The same setup was used to create positive controls for the luciferase reporter gene (LUC) assays by adding tumor necrosis factor-alpha (TNF-α, Roche; 250 ng/mL for pIL8-luc, 25 ng/mL for NFκB-luc cells) in the medium of at least three other inserts.

RESULTS

A novel humidified and thermostatized flatbed cell exposure chamber, termed NAVETTA was constructed for determination of biological responses to nanoaerosols (Figure 1). As a proof-of-principle for pro-inflammatory monitoring, two human alveolar epithelial A549 reporter cell lines were exposed to a model nanoaerosol of CuO-NPs. Particle deposition from the laminar air flow was achieved using EF and the effect on cell viability and pro-inflammatory potential was analyzed.

Characteristics of bulk NPs, Generated Nanoaerosol, And Deposited Material. The bulk material was characterized by TEM, BET surface area determination, and ICP-MS based on standardized protocols generated within the Nano-

DOI: 10.1021/acs.est.7b00493
Environ. Sci. Technol. 2017, 51, 5259−5269

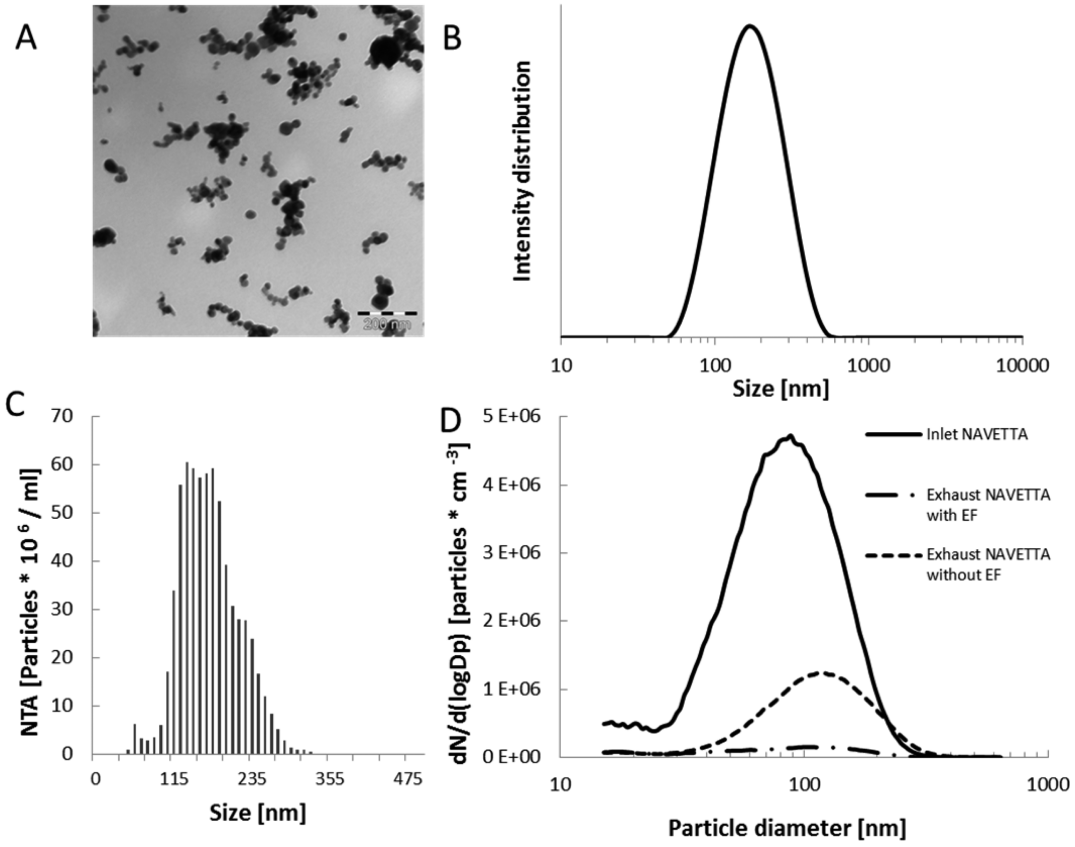

Figure 2. Physicochemical characteristics as determined by TEM (bulk material) (A), DLS (dispersion) (B, average of three independent measurements) and NTA (dispersion) (C). Generated nanoaerosol expressed as difference between particle size distribution at the inlet and exhaust (with and without EF) of the exposure chamber using the SMPS (D); Dp, particle diameter; N, particle number.

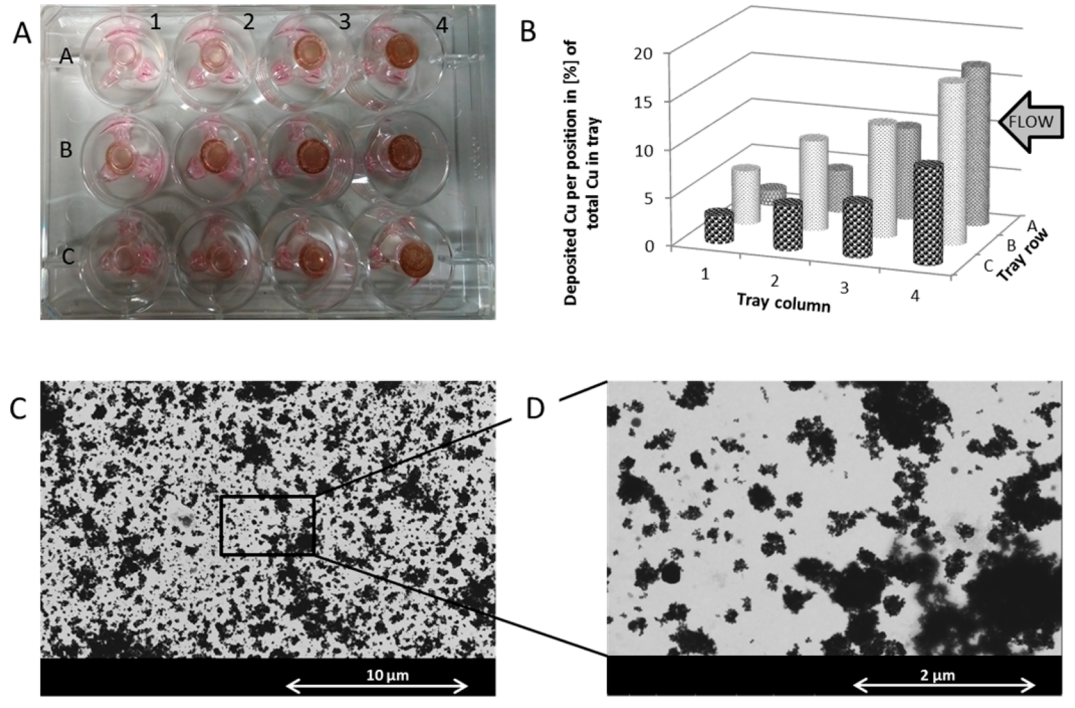

Figure 3. Quantity and agglomeration state of NAVETTA-deposited CuO. Spatial distribution of material deposited within 1 h exposure onto inverted transwell inserts as captured by photographic imaging (A) and quantified by ICP-MS (in percentage total Cu per well) (B). The flow direction is indicated by an arrow. Deposited material on position B4 was agglomerated as visualized by STEM images (20 kV) taken at 5000× (C) and 25 000× (D) magnifications, respectively.

DOI: 10.1021/acs.est.7b00493
Environ. Sci. Technol. 2017, 51, 5259−5269

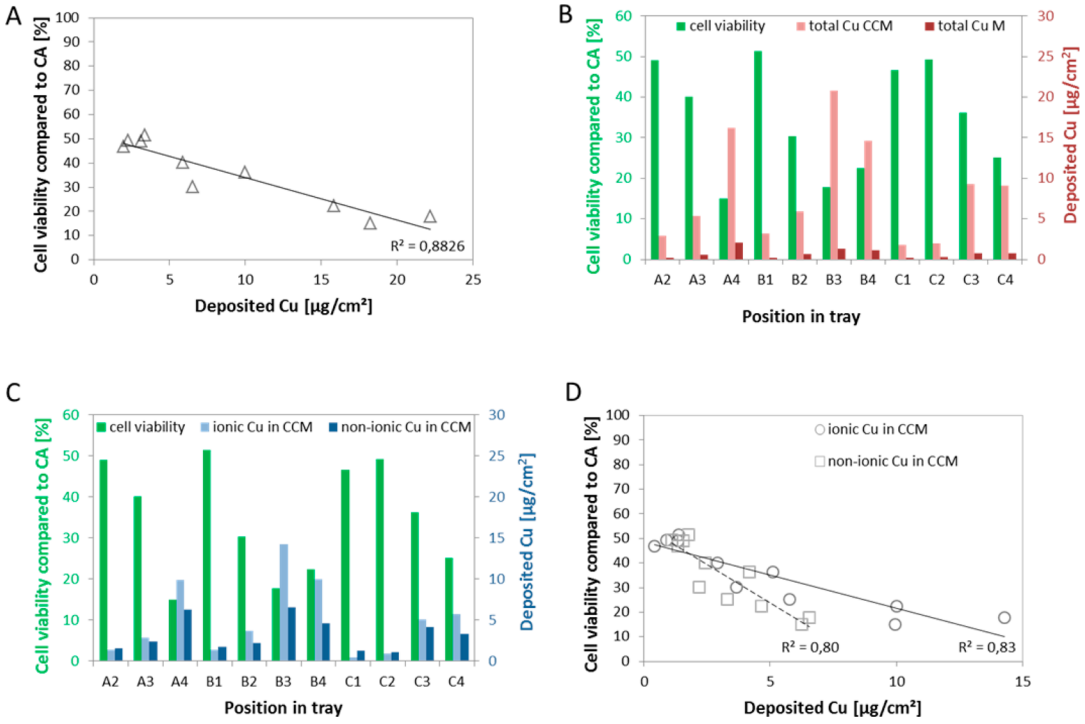

Figure 4. Scatter plot relating % cell viability of NFκB-luc cells relative to clean air (CA) to total amount of deposited Cu in cell culture medium (CCM) after 20 h postexposure incubation (A); total amounts of Cu deposited on membrane (M), or present in CCM, and % cell viability per position (B); amounts of ionic and nonionic Cu deposited in CCM and % cell viability per position (C); scatter plot relating cell viability of NFκB-luc cells and amounts of ionic (open circles, solid regression line) and nonionic (open squares, broken regression line) Cu deposited in CCM after 20 h postexposure incubation (D).

Valid consortium. The powder contained submicron-sized NP agglomerates consisting of single primary particles of 22−25 nm, with a surface area of 28 m^2/g, and purity >99% (with minor Ba and Ag contaminations). A standardized ultrasonic dispersion of CuO powder in water (4 g/L) was prepared for atomization. As depicted in Figure 2, in the CuO dispersion a primary particle size corresponding to the above-reported values was observed. Zeta potential measurements resulted in a value of +35.9 ± 1.3 mV, and DLS gave a z-average diameter of 154.5 ± 1.7 nm with a polydispersity index of 0.157. This was found to be in good agreement with a mean particle size of 168.4 ± 3.9 nm by NTA.

The nanoaerosol generated was charged and guided through the NAVETTA device for EF-assisted deposition onto cells. Particle size distribution and deposition efficiency inside the NAVETTA was determined indirectly by SMPS measurements before and after the nanoaerosol entered the chamber with and without application of the EF. Figure 2D shows the difference in particle size distribution at the inlet and exhaust of the exposure chamber with and without EF applied. The mean electrical mobility diameter was 89.1 ± 3.3 nm at the inlet, 122.0 ± 4.7 nm at the exhaust without EF applied and 102.0 ± 7.5 nm at the exhaust with EF applied. At the inlet, number concentrations of $2.7 \pm 0.3 \times 10^6$ particles·cm^{-3} were measured compared to $6.7 \pm 1.5 \times 10^5$ without EF and $1.3 \pm 0.5 \times 10^5$ particles*cm^{-3} with EF at the exhaust. Thus, deposition efficiency was approximately 95% when the EF was applied, whereas approximately 75% of the particles at the inlet deposited without application of the EF.

Visual inspection of the NAVETTA after 1 h exposure with EF revealed some degree of spatial variability of CuO among the 12 transwell positions (Figure 3A). This was also confirmed by direct quantification using ICP-MS as shown in Figure 3B. The highest total Cu concentrations were measured in the column that was reached first by the aerosol flow (column 4). All three rows (A, B, C) experienced decreasing Cu concentrations with aging flow. A preferential air flow was noticed for the row in the middle showing highest Cu concentrations in all four columns (1−4). STEM analysis of the transwell membranes after NP exposure confirmed these measurements (Figure 3C and D). Submicron-sized CuO-NP agglomerates were deposited or formed after impaction and were distributed rather homogeneously on the grid.

Suitability of NAVETTA for Investigating In Vitro Biological Responses to Nanoaerosols. Both temperature and rH values varied within a certain range as a result of opening the NAVETTA for inserting the A549 reporter cells. Immediately upon cell culture assembly, typically minimum temperature values of >33 °C were determined in the air compartment of NAVETTA. With CCM and water bath fairly constant at approximately 37 °C, the temperature in the aerial compartment adjusted quickly after reassembly. Approximately 30 min after closing the NAVETTA, rH values of >99% were again reached. Having performed preliminary tests and several follow-up optimizations, an experimental exposure condition of 1 h particle aerosolization and deposition at the ALI (inverted transwell setup), followed by postexposure incubation under submerged conditions in the cell culture incubator (20 h for cell viability, 2.5 h for pro-inflammatory potential) have been established. The mean cell viability (taking into account all positions) for both cell types was >85% after exposure to clean air in the NAVETTA versus incubator controls.

When exposing the cells to a CuO nanoaerosol flow, a decrease in cell viability of NFκB-luc cells was observed, which

DOI: 10.1021/acs.est.7b00493
Environ. Sci. Technol. 2017, 51, 5259−5269

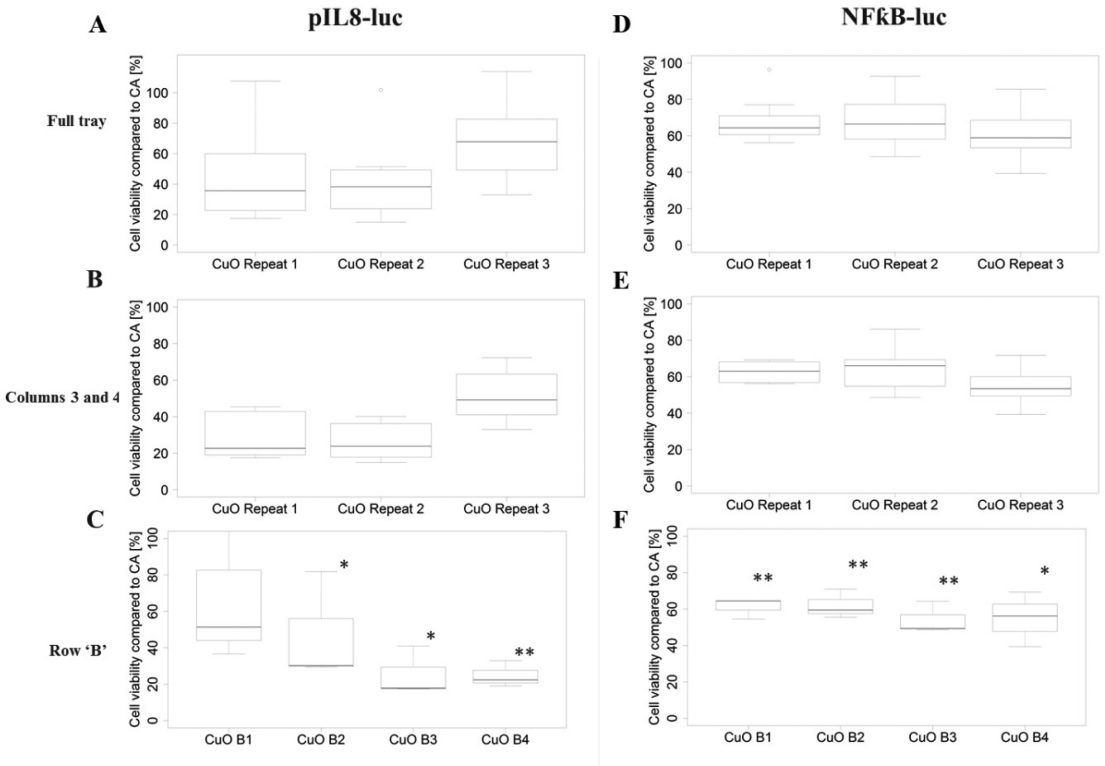

Figure 5. Cell viability (as % compared to cleanclean air, CA) of pIL8-luc (left panel) and NFκB-luc (right panel) A549 cells after 1 h exposure to CuO nanoaerosol at the ALI or CA exposure for three independent biological replicates (R1−R3). Boxplots represent analysis of the full tray (A, D), columns 3 and 4 (B, E), and individual positions of row "B" (C, F). In A B, D, and E each boxplot represents the distribution of the viability data for the 12 versus 6 cell culture inserts in the tray per replicate. In C and F each boxplot represents the distribution of the viability data for the three independent repeat experiments per position (positions B1 to B4 of tray); $*p < 0.05$; $**p \leq 0.01$; O: outliers.

correlated strongly with the increasing amount of deposited CuO material, as determined by ICP-MS (R^2 = 0.88; Figure 4A). The deposited total Cu concentration ($\mu g/cm^2$) on a transwell membrane (M) was found to be lower than the CCM Cu concentration (Figure 4B) after 20 h post incubation. This suggests that large amounts of deposited CuO on the cells were not taken up by the cells, but adsorbed at their cell membrane and transferred to the CCM during postincubation. The amounts of Cu ions released by nano-CuO into the CCM are presented in Figure 4C. Increasing total Cu concentrations resulted in increasing Cu ion concentrations in the CCM. Whether Cu ions reduce cell viability to a higher extent than nonionic Cu could not be determined from the data shown in Figure 4C and D. Notably, there was a slight but negligible difference in correlation of the decreased cell viability and ionic versus nonionic Cu concentration. Using qRT-PCR of *IL-8* mRNA, it was determined that untransfected A549 cells induce a pro-inflammatory immune response within few hours upon CuO-NPs exposure in the same low $\mu g/cm^2$ range as deposited by the NAVETTA (see SI).

Reporter Cell Viability upon Nanoaerosol Exposure in NAVETTA. To evaluate the effect of CuO-NP deposition on the viability of pIL8-luc A549 cells the CellTiter-Blueassay was used. Cell viability of the incubator controls was not significantly different (p = 0.52 and p = 0.47 for full- and half-tray analysis, respectively) compared to clean air exposure, as expected (data not shown). Figure 5A shows the cell viability percentages after 1 h exposure of pIL8-luc cells at the ALI to CuO-NPs versus clean air for 3 independent biological replicates. Each boxplot represents the distribution of the viability data for 12 cell culture inserts in the tray per replicate. It was consistently observed that CuO-NP exposure significantly ($p < 0.01$) reduced cell viability compared to clean air exposure when the 3 repeats were analyzed together. For the separate repeats, a maximum of ∼85% reduction in cell viability was observed. The same decrease in cell viability was observed after exposure to 12 ppm of NO_2 as positive control ($p < 0.01$) (data not shown). Figure 3 shows a higher CuO deposition in columns 3 and 4 and a preferential air flow in row 'B'. The half-tray analysis (Figure 5B) showed a lower variability in cell viability ($p < 0.01$) under CuO-NP exposure for the three replicates in comparison to the full-tray analysis. In Figure 5C, each boxplot represents the distribution of the viability data for 3 independent replicates per position in row B. In all B positions reduced cell viability was observed compared to clean air exposure, which was significant at position B2 (p = 0.04) and highest at positions B3 (p = 0.02) and B4 (p = 0.01).

The same CellTiter-Blueassay and analysis approach was applied for NFκB-luc A549 cells. Cell viability of the incubator controls was not significantly different (p = 0.83 and p = 0.90 for full- and half-tray analysis, respectively) compared to clean air exposure, again as expected. Figure 5D shows that CuO-NP exposure significantly ($p < 0.01$) reduced cell viability compared to clean air exposure with a maximum of ∼50% reduction of cell viability. This was also observed after NO_2 exposure ($p < 0.01$) with a maximum of ∼90% reduction in cell viability (data not shown). Evaluation of columns 3 and 4 resulted in smaller variability of the data ($p < 0.01$) in each boxplot compared to full-tray analysis (Figure 5E). In Figure

DOI: 10.1021/acs.est.7b00493
Environ. Sci. Technol. 2017, 51, 5259−5269

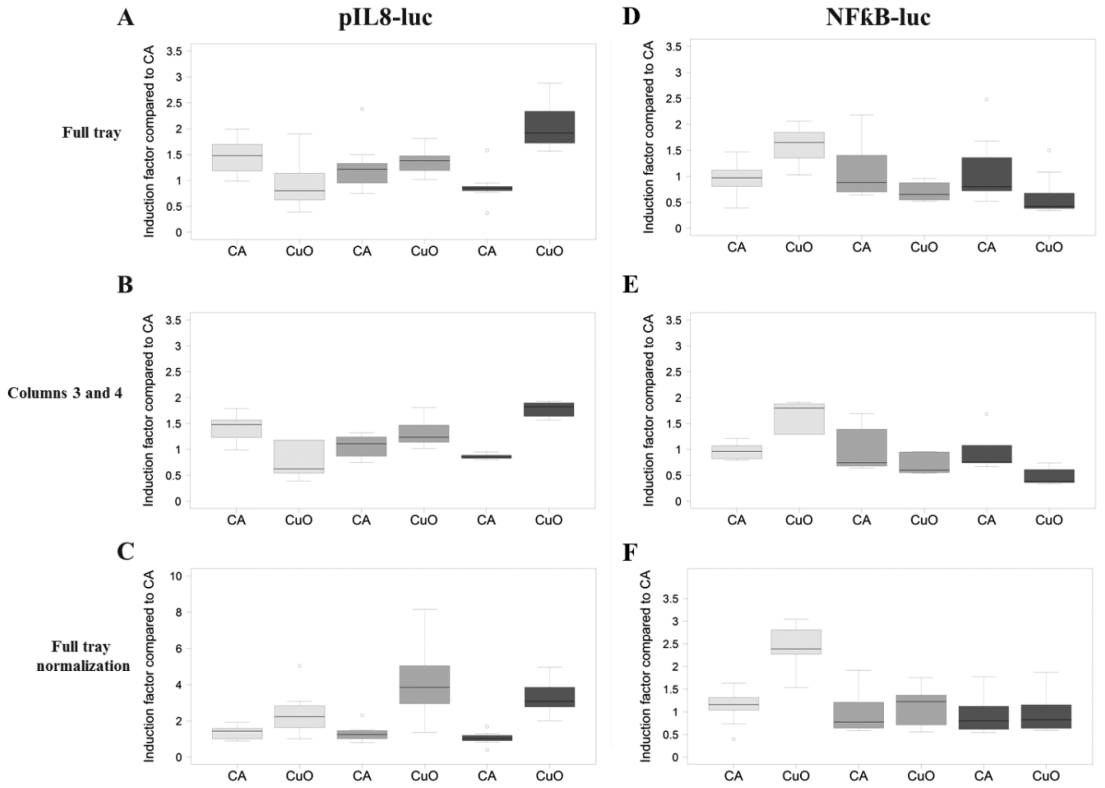

Figure 6. *IL8* promoter activity of pIL8-luc A549 cells (left panel) and NFκB activity of NFκB-luc A549 cells (right panel) after 1 h exposure to CuO nanoaerosol compared to clean air (CA) exposure for three independent biological experiments (light (repeat 1), medium (repeat 2), and dark gray (repeat 3)) for analysis of the full tray (A, D), and columns 3 and 4 (B, E). Normalization of promoter activity for % cell viability was performed in (C, F) for analysis of the full tray. O: outlier.

5F, all B positions showed significantly reduced cell viability compared to clean air exposure.

Reporter Cell Pro-Inflammatory Response to Nanoaerosol Exposure in NAVETTA. Effects of CuO nanoaerosol exposure on gene promoter activation of the pro-inflammatory cytokine IL-8 were analyzed using the stably transfected pIL8-luc A549 reporter cells. The same analysis approach was applied as for the CellTiter-Blue assay, that is, analysis of the full tray, analysis of only column 3 and 4, and only row "B". *IL8* promoter activity of the incubator controls was not significantly different (p = 0.39 and p = 0.55 for full- and half-tray analysis, respectively) compared to clean air exposure, as expected (data not shown). Figure 6A shows induction of *IL8* promoter activity after 1 h exposure to clean air versus CuO-NPs for 3 independent biological replicates. Each boxplot represents the distribution of the promoter activity data for 12 cell culture inserts in the tray per replicate. *IL8* promoter activity was decreased after CuO-NPs exposure for replicate 1, but an increase was observed for replicates 2 and 3 with a maximum induction factor ~2.9. The overall change in IL8 promoter activity after CuO-NPs exposure was statistically significantly (p = 0.04) different from clean air exposure. As a positive assay control TNF-α (250 ng/mL) was tested in parallel and was observed to induce *IL8* promoter compared to incubator controls with a factor >50 (data not shown). Evaluation of columns 3 and 4 (i.e., six technical replicates) resulted in a smaller variability of the data (p = 0.21) compared to full-tray analysis (Figure 6B). No change in *IL8* promoter activity was observed for all B positions (data not shown).

Assuming that cells that are still viable after 20 h postexposure incubation contribute most to *IL8* promoter induction after 2.5 h postexposure incubation, we normalized the data of *IL8* promoter activity for % cell viability. Figure 6C shows a significantly (p < 0.01) increased *IL8* promoter activity after CuO-NP exposure compared to clean air for all three replicates.

The same LUC assay and analysis approach was applied for NFκB-luc A549 cells which allows evaluating effects on induction of *NFκB* response elements. NFκB activity of the incubator controls was not significantly different (p = 0.44 and p = 0.08 for full- and half-tray analysis, respectively) compared to clean air exposure, as expected. Figure 6D shows NFκB activity after 1 h exposure to clean air versus CuO-NP for 3 independent biological replicates. NFκB activity increased after CuO-NP exposure compared to clean air exposure for replicate 1, but a decrease was observed for replicates 2 and 3. The overall change in NFκB activity after CuO-NP exposure was not significantly (p = 0.44) different from clean air exposure. The positive control TNF-α (25 ng/mL)) induced *NFκB* compared to clean air with a factor >3 (data not shown). Evaluation of columns 3 and 4 resulted in a smaller variability of the data in each boxplot compared to full-tray analysis (p = 0.77) (Figure 6E). No change in NFκB activity was observed for all B positions (data not shown). Also here, NFκB activity assessed after 2.5 h postexposure was normalized for % cell viability (determined after 20 h postexposure incubation). Figure 6F shows an increased NFκB activity, in particular for replicate 1. Overall, a significantly increased (p < 0.01) NFκB activity after CuO-NPs exposure compared to clean air for all 3 replicates was found.

DOI: 10.1021/acs.est.7b00493
Environ. Sci. Technol. 2017, 51, 5259−5269

DISCUSSION

The current study is a follow-up of Stoehr et al.[13] reporting on biological effects observed upon EF-assisted deposition of a diesel exhaust aerosol using a cylindrically shaped acryl glass precursor exposure chamber without control of temperature, humidity, and aerosol turbulences. In order to improve the deposition efficiency, a novel humidified and thermostatized flatbed cell exposure chamber was constructed for in vitro cell exposure and fast and simple determination of biological responses to nanoaerosols (Figure 1). Two human alveolar epithelial A549 reporter cell lines cultured on an inverted ALI setup for assessing triggering of pro-inflammatory IL-8 and NFκB pathways were used for exposure to a nanoaerosol of CuO-NPs. Efficient NP deposition from the laminar air flow was mediated by EF, and the effect on cell viability and pro-inflammatory potential was analyzed by direct read-out of luminescence. Importantly, the generated nanoaerosol was thoroughly characterized during all experimental steps from the primary CuO-NPs using TEM, upon dispersion in water by DLS and NTA, upon aerosolization with/without EF applied by SMPS, and finally after deposition by SEM and ICP-MS. During optimization of the exposure conditions, different exposure times, ranging from 30 min to several hours, and several postincubation periods, up to 24 h, were tested in terms of cell viability and variance between different positions. No long-term stability of the inverted ALI setup was achieved, most probably due to the lower hydrostatic pressure of the CCM in the inverted compared to normal ALI setup by which cells were not sufficiently supplied with nutrients. For establishing stable pH conditions, required for optimal cell viability under exposure conditions of inverted ALI-cultured reporter cells, 25 mM HEPES buffer was included in the CCM. The nanoaerosol was generated by atomization from well-characterized CuO-NPs dispersed by ultrasonication under reproducible conditions strictly following a SOP carefully elaborated within the European Union NanoValid project (www.nanovalid.eu). Atomization from the wet state was selected from different aerosolization techniques in order to achieve highest deposition efficiency and minimal particle agglomeration of the aerosol. It enabled higher particle number concentrations within the nanosized range compared to dry generation producing fewer particles of a bigger size due to agglomeration. Improvement of NP polydispersity following atomization was investigated by using electrospray aerosol generation, but this turned out inadequate due to precipitation of CuO in suitable buffer solutions. Upon drying the nanoaerosol after atomization, the CuO-NPs were charged and deposited using EF assistance, a procedure which represents a common technique in particle aerosol studies in vitro[63,64] and which we previously used for intrinsically charged diesel exhaust particles.[13] Notably, the deposition efficiency of ∼75% obtained without EF in the NAVETTA exceeded the value previously reported for 25 nm Cu-CuO_2 core−shell NPs using impaction-mediated deposition,[10] while using EF assistance this value could be increased to ∼95% in our study.

Several construction optimization steps were done to obtain maximal nanoaerosol deposition. A water bath was used and found to be sufficient for chamber humidification, which was monitored by cell viability and baseline reporter responses. To avoid losses of NPs in the water bath a metal bridge was included for separating the humidification and deposition compartments, optimized in width to provide a laterally most even spatial nanoaerosol distribution upon EF application. Still, a longitudinal gradient of deposited material was observed (determined by ICP-MS), which seems useful for the acquisition of dose−response curves when optimized in future. Special stub electrodes underneath the cells inside a SS tray, a counter electrode on the opposite side, and a polystyrene lid to circumvent CuO-NPs loss into the CCM established a highly directed EF-assisted deposition onto the ALI-cultured reporter cells within short time. As evidenced by cell viability and baseline reporter responses, the applied EF per se did not affect the cells. We found that due to the laminar aerosol flow and the inverted orientation of transwells, much higher deposition rates were obtained compared to a normal ALI setup.

After 1 h exposure to the CuO nanoaerosol, the cells were submerged again for postexposure incubation (2.5 h for LUC assay, 20 h for CTB assay) required for the induction of cellular responses. During the postincubation period of 20 h, CuO-NPs dissolved in a concentration-dependent manner, as determined using ICP-MS (Figure 4D). Thus, the observed cytotoxicity observed in our study seems to be a result of both fractions, the ionic and nonionic fraction. It has been reported before that toxicity of CuO-NPs depends on dissolution, at least to a significant extent.[59−61,65,66]

Using the optimized inverted ALI exposure and post-incubation setup described here, pro-inflammatory immune responses, in terms of *IL8* promoter and NFκB activity, were observed within a short time, that is, One hour exposure to ALI-deposited CuO-NPs and 2.5 h postincubation. Immune activity read-outs displayed less pronounced effects upon CuO-NP exposure at the ALI compared to the marked reduction in viability, and higher variabilities were found. Thus, further construction optimizations (e.g., leak tightness, flow path) will be needed to enhance reproducibility and reduce spatial variability when measuring immune responses resulting from nanoaerosol exposure. Nevertheless, upon normalization for cell viability (Figure 6C), statistically significant pro-inflammatory effects were detectable in the low microgram range of deposited material. To corroborate these results we tested for *IL8* mRNA transcription in untransfected A549 cells cultured under submerged conditions using qRT-PCR and found that the low $\mu g/cm^2$ amounts of CuO-NPs necessary for inducing a pro-inflammatory response within these exposure periods correlated well with the data obtained from NAVETTA-exposed reporter cells (see SI).

In conclusion, the flatbed aerosol exposure chamber NAVETTA is capable of mimicking more realistic human lung cell exposure to nanoparticles compared to other ALI systems. Commercially available ALI exposure systems like VITROCELL,[67] CULTEX,[68] and P.R.I.T.[69] expose cells seeded in normal transwell ALI setup to a perpendicular flow, while NAVETTA is designed for a horizontal flow combined with cells cultured in an inverted transwell ALI setup. Natural conditioning (humidification and warming) of the aerosol flow being delivered to the cells is achieved with a water bath and Peltier elements, minimizing lung cell damage. In-line conditioning of the aerosol flow is not commonly integrated in commercially available systems, but is often added as an independent component when it is used. A common phenomenon in normal transwell ALI setup is flooding of the cell surface with CCM due to hydrostatic pressure which neutralizes the ALI advantage. The inverted transwell ALI setup used in the NAVETTA prevents this from happening, but so far shows limited stability that can be overcome when combining

DOI: 10.1021/acs.est.7b00493
Environ. Sci. Technol. 2017, 51, 5259−5269

the setup with rapid biological read-out systems, such as reported cell lines.

The major progress of the present study is to highly efficiently and directly deposit a charged metal oxide nanoaerosol supplied in a low laminar horizontal flow onto reporter cells, and to read-out immune responses within short-term. Exposure conditions were optimized for cellular performance and to mimic an exposure scenario as realistic as possible to the situation in the human lung. Currently the NAVETTA is operated at a nominal rate preset by the SMPS' intrinsic operational flow rate of 0.3 lpm. By adjusting the throughput to higher or lower rates, the NAVETTA is able to mimic lung depositions that cover the wider bronchial as well as the acinar regime. The NAVETTA device has features that can complement existing test options for assessing toxicity of nanoparticles upon inhalation.

■ ASSOCIATED CONTENT

Supporting Information

The Supporting Information is available free of charge on the ACS Publications website at DOI: 10.1021/acs.est.7b00493.

Further methods in greater detail and supplementary results, i.e., IL-8 qRT-PCR upon CuO exposure of untransfected A549 cells in submerged culture, depicted in Figure S1(PDF)

■ AUTHOR INFORMATION

Corresponding Author

*Phone: +43 662 8044 5713; fax: +43 662 8044 5751; e-mail: martin.himly@sbg.ac.at.

ORCID

Albert Duschl: 0000-0002-7034-9860

Martin Himly: 0000-0001-5416-085X

Notes

The authors declare no competing financial interest.

■ ACKNOWLEDGMENTS

This research has received funding from the European Union (EU) Seventh Framework Programme (FP7/2007-2013) Grant Agreement No. 263147 (NanoValid − Development of reference methods for hazard identification, risk assessment and LCA of engineered nanomaterials). We are grateful to Peter Lanner (www.lanner-maschinenbau.com) for technical support when engineering NAVETTA and Hanny Willems (VITO) for statistical support.

■ REFERENCES

(1) Paur, H. R.; Cassee, F. R.; Teeguarden, J.; Fissan, H.; Diabate, S.; Aufderheide, M.; Kreyling, W.; Hänninen, O.; Kasper, G.; Riediker, M.; Rothen-Rutishauser, B.; Schmid, O. In vitro cell exposure studies for the assessment of nanoparticle toxicity in the lung - a dialogue between aerosol science and biology. *J. Aerosol Sci.* **2011**, *42*, 668−692.

(2) Müller, L.; Gasser, M.; Raemy, D. O.; Herzog, F.; Brandenberger, C.; Schmid, O. Realistic exposure methods for investigating the interaction of nanoparticles with the lung at the air-liquid interface in vitro. *Insci. J.* **2011**, *1*, 30−64.

(3) Aufderheide, M. An efficient approach to study the toxicological effects of complex mixtures. *Exp. Toxicol. Pathol.* **2008**, *60* (2−3), 163−180.

(4) Bitterle, E.; Karg, E.; Schroeppel, A.; Kreyling, W. G.; Tippe, A.; Ferron, G. A.; Schmid, O.; Heyder, J.; Maier, K. L.; Hofer, T. Dose-controlled exposure of A549 epithelial cells at the air-liquid interface to airborne ultrafine carbonaceous particles. *Chemosphere* **2006**, *65* (10), 1784−1790.

(5) Diabate, S.; Mulhopt, S.; Paur, H. R.; Krug, H. F. The response of a co-culture lung model to fine and ultrafine particles of incinerator fly ash at the air-liquid interface. *Altern. Lab Anim* **2008**, *36* (3), 285−298.

(6) Lenz, A. G.; Karg, E.; Lentner, B.; Dittrich, V.; Brandenberger, C.; Rothen-Rutishauser, B.; Schulz, H.; Ferron, G. A.; Schmid, O. A dose-controlled system for air-liquid interface cell exposure and application to zinc oxide nanoparticles. *Part. Fibre Toxicol.* **2009**, *6*, 32.

(7) Rothen-Rutishauser, B.; Grass, R. N.; Blank, F.; Limbach, L. K.; Muhlfeld, C.; Brandenberger, C.; Raemy, D. O.; Gehr, P.; Stark, W. J. Direct combination of nanoparticle fabrication and exposure to lung cell cultures in a closed setup as a method to simulate accidental nanoparticle exposure of humans. *Environ. Sci. Technol.* **2009**, *43* (7), 2634−2640.

(8) Steinritz, D.; Mohle, N.; Pohl, C.; Papritz, M.; Stenger, B.; Schmidt, A.; Kirkpatrick, C. J.; Thiermann, H.; Vogel, R.; Hoffmann, S.; Aufderheide, M. Use of the Cultex(R) Radial Flow System as an in vitro exposure method to assess acute pulmonary toxicity of fine dusts and nanoparticles with special focus on the intra- and inter-laboratory reproducibility. *Chem.-Biol. Interact.* **2013**, *206* (3), 479−490.

(9) Klein, S. G.; Serchi, T.; Hoffmann, L.; Blomeke, B.; Gutleb, A. C. An improved 3D tetraculture system mimicking the cellular organisation at the alveolar barrier to study the potential toxic effects of particles on the lung. *Part. Fibre Toxicol.* **2013**, *10*, 31.

(10) Kim, J. S.; Peters, T. M.; O'Shaughnessy, P. T.; Adamcakova-Dodd, A.; Thorne, P. S. Validation of an in vitro exposure system for toxicity assessment of air-delivered nanomaterials. *Toxicol. In Vitro* **2013**, *27* (1), 164−73.

(11) Volckens, J.; Dailey, L.; Walters, G.; Devlin, R. B. Direct particle-to-cell deposition of coarse ambient particulate matter increases the production of inflammatory mediators from cultured human airway epithelial cells. *Environ. Sci. Technol.* **2009**, *43* (12), 4595−4599.

(12) de, B. K.; Ebersviller, S.; Sexton, K. G.; Lake, S.; Leith, D.; Goodman, R.; Jetters, J.; Walters, G. W.; Doyle-Eisele, M.; Woodside, R.; Jeffries, H. E.; Jaspers, I. Design and testing of Electrostatic Aerosol in Vitro Exposure System (EAVES): an alternative exposure system for particles. *Inhalation Toxicol.* **2009**, *21* (2), 91−101.

(13) Stoehr, L. C.; Madl, P.; Boyles, M. S.; Zauner, R.; Wimmer, M.; Wiegand, H.; Andosch, A.; Kasper, G.; Pesch, M.; Lutz-Meindl, U.; Himly, M.; Duschl, A. Enhanced Deposition by Electrostatic Field-Assistance Aggravating Diesel Exhaust Aerosol Toxicity for Human Lung Cells. *Environ. Sci. Technol.* **2015**, *49* (14), 8721−8730.

(14) Panas, A.; Comouth, A.; Saathoff, H.; Leisner, T.; Al-Rawi, M.; Simon, M.; Seemann, G.; Dossel, O.; Mulhopt, S.; Paur, H. R.; Fritsch-Decker, S.; Weiss, C.; Diabate, S. Silica nanoparticles are less toxic to human lung cells when deposited at the air-liquid interface compared to conventional submerged exposure. *Beilstein J. Nanotechnol.* **2014**, *5*, 1590−1602.

(15) Cooney, D. J.; Hickey, A. J. Cellular response to the deposition of diesel exhaust particle aerosols onto human lung cells grown at the air-liquid interface by inertial impaction. *Toxicol. In Vitro* **2011**, *25* (8), 1953−1965.

(16) Holder, A. L.; Lucas, D.; Goth-Goldstein, R.; Koshland, C. P. Inflammatory response of lung cells exposed to whole, filtered, and hydrocarbon denuded diesel exhaust. *Chemosphere* **2007**, *70* (1), 13−19.

(17) Hawley, B.; McKenna, D.; Marchese, A.; Volckens, J. Time course of bronchial cell inflammation following exposure to diesel particulate matter using a modified EAVES. *Toxicol. In Vitro* **2014**, *28* (5), 829−837.

(18) Holder, A. L.; Lucas, D.; Goth-Goldstein, R.; Koshland, C. P. Cellular response to diesel exhaust particles strongly depends on the exposure method. *Toxicol. Sci.* **2008**, *103* (1), 108−115.

(19) Kooter, I. M.; Albias, M. J.; Jedynska, A. D.; Steenhof, M.; Houtzager, M. M.; van, R. M. Alveolar epithelial cells (A549) exposed at the air-liquid interface to diesel exhaust: First study in TNO's powertrain test center. *Toxicol. In Vitro* **2013**, *27* (8), 2342−2349.

DOI: 10.1021/acs.est.7b00493
Environ. Sci. Technol. 2017, 51, 5259−5269

(20) Oostingh, G. J.; Papaioannou, E.; Chasapidis, L.; Akritidis, T.; Konstandopoulos, A. G.; Duschl, A. Development of an on-line exposure system to determine freshly produced diesel engine emission-induced cellular effects. *Toxicol. In Vitro* **2013**, *27* (6), 1746−1752.
(21) Seagrave, J.; Dunaway, S.; McDonald, J. D.; Mauderly, J. L.; Hayden, P.; Stidley, C. Responses of differentiated primary human lung epithelial cells to exposure to diesel exhaust at an air-liquid interface. *Exp. Lung Res.* **2007**, *33* (1), 27−51.
(22) Tsukue, N.; Okumura, H.; Ito, T.; Sugiyama, G.; Nakajima, T. Toxicological evaluation of diesel emissions on A549 cells. *Toxicol. In Vitro* **2010**, *24* (2), 363−369.
(23) Lam, H. C.; Choi, A. M.; Ryter, S. W., Isolation of mouse respiratory epithelial cells and exposure to experimental cigarette smoke at air liquid interface. *J. Visualized Exp.* **2011**, (48.10.3791/2513
(24) Mathis, C.; Poussin, C.; Weisensee, D.; Gebel, S.; Hengstermann, A.; Sewer, A.; Belcastro, V.; Xiang, Y.; Ansari, S.; Wagner, S.; Hoeng, J.; Peitsch, M. C. Human bronchial epithelial cells exposed in vitro to cigarette smoke at the air-liquid interface resemble bronchial epithelium from human smokers. *Am. J. Physiol Lung Cell Mol. Physiol* **2013**, *304* (7), L489−L503.
(25) Brandenberger, C.; Rothen-Rutishauser, B.; Muhlfeld, C.; Schmid, O.; Ferron, G. A.; Maier, K. L.; Gehr, P.; Lenz, A. G. Effects and uptake of gold nanoparticles deposited at the air-liquid interface of a human epithelial airway model. *Toxicol. Appl. Pharmacol.* **2010**, *242* (1), 56−65.
(26) Elihn, K.; Cronholm, P.; Karlsson, H. L.; Midander, K.; Odnevall, W. I; Muller, L. Cellular dose of partly soluble Cu particle aerosols at the air-liquid interface using an in vitro lung cell exposure system. *J. Aerosol Med. Pulm. Drug Delivery* **2013**, *26* (2), 84−93.
(27) Grigg, J.; Tellabati, A.; Jones, G. D.; Howes, P. DNA damage of macrophages induced by metal nanoparticulates using an air-liquid interface exposure model. *Nanotoxicology* **2013**, *7* (5), 961−962.
(28) Herzog, F.; Clift, M. J.; Piccapietra, F.; Behra, R.; Schmid, O.; Petri-Fink, A.; Rothen-Rutishauser, B. Exposure of silver-nanoparticles and silver-ions to lung cells in vitro at the air-liquid interface. *Part. Fibre Toxicol.* **2013**, *10*, 11.
(29) Holder, A. L.; Marr, L. C. Toxicity of silver nanoparticles at the air-liquid interface. *BioMed Res. Int.* **2013**, *2013*, 328934.
(30) Lenz, A. G.; Karg, E.; Brendel, E.; Hinze-Heyn, H.; Maier, K. L.; Eickelberg, O.; Stoeger, T.; Schmid, O. Inflammatory and oxidative stress responses of an alveolar epithelial cell line to airborne zinc oxide nanoparticles at the air-liquid interface: a comparison with conventional, submerged cell-culture conditions. *BioMed Res. Int.* **2013**, *2013*, 652632.
(31) Mihai, C.; Chrisler, W. B.; Xie, Y.; Hu, D.; Szymanski, C. J.; Tolic, A.; Klein, J. A.; Smith, J. N.; Tarasevich, B. J.; Orr, G. Intracellular accumulation dynamics and fate of zinc ions in alveolar epithelial cells exposed to airborne ZnO nanoparticles at the air-liquid interface. *Nanotoxicology* **2015**, *9* (1), 9−22.
(32) Stoehr, L. C.; Endes, C.; Radauer-Preiml, I.; Boyles, M. S.; Casals, E.; Balog, S.; Pesch, M.; Petri-Fink, A.; Rothen-Rutishauser, B.; Himly, M.; Clift, M. J.; Duschl, A. Assessment of a panel of interleukin-8 reporter lung epithelial cell lines to monitor the pro-inflammatory response following zinc oxide nanoparticle exposure under different cell culture conditions. *Part. Fibre Toxicol.* **2015**, *12*, 29.
(33) Xie, Y.; Williams, N. G.; Tolic, A.; Chrisler, W. B.; Teeguarden, J. G.; Maddux, B. L.; Pounds, J. G.; Laskin, A.; Orr, G. Aerosolized ZnO nanoparticles induce toxicity in alveolar type II epithelial cells at the air-liquid interface. *Toxicol. Sci.* **2012**, *125* (2), 450−461.
(34) Savi, M.; Kalberer, M.; Lang, D.; Ryser, M.; Fierz, M.; Gaschen, A.; Ricka, J.; Geiser, M. A novel exposure system for the efficient and controlled deposition of aerosol particles onto cell cultures. *Environ. Sci. Technol.* **2008**, *42* (15), 5667−5674.
(35) Stevens, J. P.; Zahardis, J.; MacPherson, M.; Mossman, B. T.; Petrucci, G. A. A new method for quantifiable and controlled dosage of particulate matter for in vitro studies: the electrostatic particulate dosage and exposure system (EPDExS). *Toxicol. In Vitro* **2008**, *22* (7), 1768−1774.
(36) Wieder, K. J.; King, K. R.; Thompson, D. M.; Zia, C.; Yarmush, M. L.; Jayaraman, A. Optimization of reporter cells for expression profiling in a microfluidic device. *Biomed. Microdevices* **2005**, *7* (3), 213−222.
(37) Vishwanath, R. P.; Brown, C. E.; Wagner, J. R.; Meechoovet, H. B.; Naranjo, A.; Wright, C. L.; Olivares, S.; Qian, D.; Cooper, L. J.; Jensen, M. C. A quantitative high-throughput chemotaxis assay using bioluminescent reporter cells. *J. Immunol. Methods* **2005**, *302* (1−2), 78−89.
(38) Westerink, W. M.; Stevenson, J. C.; Horbach, G. J.; Schoonen, W. G. The development of RAD51C, Cystatin A, p53 and Nrf2 luciferase-reporter assays in metabolically competent HepG2 cells for the assessment of mechanism-based genotoxicity and of oxidative stress in the early research phase of drug development. *Mutat. Res., Genet. Toxicol. Environ. Mutagen.* **2010**, *696* (1), 21−40.
(39) Karlsson, H. L.; Gliga, A. R.; Calleja, F. M.; Goncalves, C. S.; Wallinder, I. O.; Vrieling, H.; Fadeel, B.; Hendriks, G. Mechanism-based genotoxicity screening of metal oxide nanoparticles using the ToxTracker panel of reporter cell lines. *Part. Fibre Toxicol.* **2014**, *11*, 41.
(40) Chen, P.; Kanehira, K.; Sonezaki, S.; Taniguchi, A. Detection of cellular response to titanium dioxide nanoparticle agglomerates by sensor cells using heat shock protein promoter. *Biotechnol. Bioeng.* **2012**, *109* (12), 3112−3118.
(41) Jammi, S.; Sakthivel, S.; Rout, L.; Mukherjee, T.; Mandal, S.; Mitra, R.; Saha, P.; Punniyamurthy, T. CuO nanoparticles catalyzed C-N, C-O, and C-S cross-coupling reactions: scope and mechanism. *J. Org. Chem.* **2009**, *74* (5), 1971−1976.
(42) Chowdhuri, A.; Gupta, V.; Sreenivas, K.; Kumar, R.; Mozumdar, S.; Patanjali, P. K. Response speed of SnO2-based gas sensors with CuO nanoparticles. *Appl. Phys. Lett.* **2004**, *84*, 1180−1182.
(43) Zhang, D. W.; Yi, T. H.; Chen, C. H. Cu nanoparticles derived from CuO electrodes in lithium cells. *Nanotechnology* **2005**, *16* (10), 2338−2341.
(44) Yin, M.; Wu, C. K.; Lou, Y.; Burda, C.; Koberstein, J. T.; Zhu, Y.; O'Brien, S. Copper oxide nanocrystals. *J. Am. Chem. Soc.* **2005**, *127* (26), 9506−9511.
(45) Dar, M. A.; Kim, Y. S.; Kim, W. B.; Sohn, J. M.; Shin, H. S. Structural and magnetic properties of CuO nanoneedles synthesized by hydrothermal method. *Appl. Surf. Sci.* **2008**, *254*, 7477−7481.
(46) Ren, G.; Hu, D.; Cheng, E. W.; Vargas-Reus, M. A.; Reip, P.; Allaker, R. P. Characterisation of copper oxide nanoparticles for antimicrobial applications. *Int. J. Antimicrob. Agents* **2009**, *33* (6), 587−590.
(47) Chang, Y. N.; Zhang, M.; Xia, L.; Zhang, J.; Xing, G. The toxic effects and mechanisms of CuO and ZnO nanoparticles. *Materials* **2012**, *5*, 2850−2871.
(48) Galhardi, C. M.; Diniz, Y. S.; Rodrigues, H. G.; Faine, L. A.; Burneiko, R. C.; Ribas, B. O.; Novelli, E. L. Beneficial effects of dietary copper supplementation on serum lipids and antioxidant defenses in rats. *Ann. Nutr. Metab.* **2005**, *49* (5), 283−288.
(49) Zietz, B. P.; Dieter, H. H.; Lakomek, M.; Schneider, H.; Kessler-Gaedtke, B.; Dunkelberg, H. Epidemiological investigation on chronic copper toxicity to children exposed via the public drinking water supply. *Sci. Total Environ.* **2003**, *302* (1−3), 127−144.
(50) Yokohira, M.; Kuno, T.; Yamakawa, K.; Hosokawa, K.; Matsuda, Y.; Hashimoto, N.; Suzuki, S.; Saoo, K.; Imaida, K. Lung toxicity of 16 fine particles on intratracheal instillation in a bioassay model using f344 male rats. *Toxicol. Pathol.* **2008**, *36* (4), 620−631.
(51) Ahamed, M.; Siddiqui, M. A.; Akhtar, M. J.; Ahmad, I.; Pant, A. B.; Alhadlaq, H. A. Genotoxic potential of copper oxide nanoparticles in human lung epithelial cells. *Biochem. Biophys. Res. Commun.* **2010**, *396* (2), 578−583.
(52) Akhtar, M. J.; Kumar, S.; Alhadlaq, H. A.; Alrokayan, S. A.; Abu-Salah, K. M.; Ahamed, M. Dose-dependent genotoxicity of copper oxide nanoparticles stimulated by reactive oxygen species in human lung epithelial cells. *Toxicol. Ind. Health* **2013**, *32* (5), 809−21.

DOI: 10.1021/acs.est.7b00493
Environ. Sci. Technol. 2017, 51, 5259−5269

(53) Fahmy, B.; Cormier, S. A. Copper oxide nanoparticles induce oxidative stress and cytotoxicity in airway epithelial cells. *Toxicol. In Vitro* **2009**, *23* (7), 1365−1371.
(54) Karlsson, H. L.; Cronholm, P.; Gustafsson, J.; M?ller, L. Copper oxide nanoparticles are highly toxic: a comparison between metal oxide nanoparticles and carbon nanotubes. *Chem. Res. Toxicol.* **2008**, *21* (9), 1726−1732.
(55) Midander, K.; Cronholm, P.; Karlsson, H. L.; Elihn, K.; M?ller, L.; Leygraf, C.; Wallinder, I. O. Surface characteristics, copper release, and toxicity of nano- and micrometer-sized copper and copper(II) oxide particles: a cross-disciplinary study. *Small* **2009**, *5* (3), 389−399.
(56) Wang, Z.; Li, N.; Zhao, J.; White, J. C.; Qu, P.; Xing, B. CuO nanoparticle interaction with human epithelial cells: cellular uptake, location, export, and genotoxicity. *Chem. Res. Toxicol.* **2012**, *25* (7), 1512−1521.
(57) Karlsson, H. L.; Gustafsson, J.; Cronholm, P.; M?ller, L. Size-dependent toxicity of metal oxide particles–a comparison between nano- and micrometer size. *Toxicol. Lett.* **2009**, *188* (2), 112−118.
(58) Sun, J.; Wang, S.; Zhao, D.; Hun, F. H.; Weng, L.; Liu, H. Cytotoxicity, permeability, and inflammation of metal oxide nanoparticles in human cardiac microvascular endothelial cells: cytotoxicity, permeability, and inflammation of metal oxide nanoparticles. *Cell Biol. Toxicol.* **2011**, *27* (5), 333−342.
(59) Piret, J. P.; Vankoningsloo, S.; Mejia, J.; Noel, F.; Boilan, E.; Lambinon, F.; Zouboulis, C. C.; Masereel, B.; Lucas, S.; Saout, C.; Toussaint, O. Differential toxicity of copper (II) oxide nanoparticles of similar hydrodynamic diameter on human differentiated intestinal Caco-2 cell monolayers is correlated in part to copper release and shape. *Nanotoxicology* **2012**, *6* (7), 789−803.
(60) Semisch, A.; Ohle, J.; Witt, B.; Hartwig, A. Cytotoxicity and genotoxicity of nano - and microparticulate copper oxide: role of solubility and intracellular bioavailability. *Part. Fibre Toxicol.* **2014**, *11*, 10.
(61) Moschini, E.; Gualtieri, M.; Colombo, M.; Fascio, U.; Camatini, M.; Mantecca, P. The modality of cell-particle interactions drives the toxicity of nanosized CuO and TiO(2) in human alveolar epithelial cells. *Toxicol. Lett.* **2013**, *222* (2), 102−116.
(62) Oostingh, G. J.; Schmittner, M.; Ehart, A. K.; Tischler, U.; Duschl, A. A high-throughput screening method based on stably transformed human cells was used to determine the immunotoxic effects of fluoranthene and other PAHs. *Toxicol. In Vitro* **2008**, *22* (5), 1301−1310.
(63) Fierz, M.; Houle, C.; Steigmeier, P.; Burtscher, H. Design, calibration, and field performance of a miniature diffusion size classifier. *Aerosol Sci. Technol.* **2011**, *45* (1), 1−10.
(64) Marra, J.; Voetz, M.; Kiesling, H. J. Monitor for detecting and assessing exposure to airborne nanoparticles. *J. Nanopart. Res.* **2016**, *12* (1), 21−37.
(65) Boyles, M. S. P.; Ranninger, C.; Reischl, R.; Rurik, M.; Tessardri, R.; Kohlbacher, O.; Duschl, A.; Huber, C. G. Copper oxide nanoparticle toxicity profiling using untargeted metabolomics. *Part. Fibre Toxicol.* **2015**, *13* (1), 49.
(66) Cronholm, P.; Karlsson, H. L.; Hedberg, J.; Lowe, T. A.; Winnberg, L.; Elihn, K.; Wallinder, I. O.; M?ller, L. Intracellular uptake and toxicity of Ag and CuO nanoparticles: a comparison between nanoparticles and their corresponding metal ions. *Small* **2013**, *9* (7), 970−982.
(67) Aufderheide, M.; Mohr, U. A modified CULTEX system for the direct exposure of bacteria to inhalable substances. *Exp. Toxicol. Pathol.* **2004**, *55* (6), 451−454.
(68) Aufderheide, M.; Mohr, U. CULTEX–a new system and technique for the cultivation and exposure of cells at the air/liquid interface. *Exp. Toxicol. Pathol.* **1999**, *51* (6), 489−490.
(69) Ritter, D.; Knebel, J. W., Investigations of the biological effects of airborne and inhalable substances by cell-based in vitro methods: fundamental improvements to the ALI concept. *Advances in Toxicology* **2014**, *2014*, Article ID 185201.110.1155/2014/185201

DOI: 10.1021/acs.est.7b00493
Environ. Sci. Technol. 2017, 51, 5259−5269